# High-pressure high-temperature synthesis of non-centrosymmetric R3Pt4Ge13 compounds with R = Gd, Dy, Ho, Er and Lu

Christine Opagiste, Rose-Marie Galéra, M. Legendre, C. Goujon, S. Pairis, P. Bordet

# High-pressure high-temperature synthesis of non-centrosymmetric $R_3Pt_4Ge_{13}$ compounds with $R$ = Gd, Dy, Ho, Er and Lu

C. Opagiste*, R.-M. Galéra, M. Legendre, C. Goujon, S. Pairis and P. Bordet

Institut Néel, Univ. Grenoble Alpes, CNRS, Grenoble INP, 38000 Grenoble, France

*Corresponding author email address: christine.opagiste@neel.cnrs.fr (C. Opagiste)

**Abstract**

New compounds of composition $R_3Pt_4Ge_{13}$ have been successfully prepared with $R$ = Dy, Ho, Er and Lu, by high-pressure (5 - 7 GPa) and high-temperature synthesis (up to 1073 K). Structural analysis confirms that all compounds crystallize in a non-centrosymmetric monoclinic structure (space group *Cc*). The magnetic properties of these four new compounds were studied, as well as those of $Gd_3Pt_4Ge_{13}$, a known compound on which few physical studies have been published. The magnetic susceptibility of the Gd, Dy, Ho and Er compounds follow a Curie-Weiss law in the temperature range 20 K - 300 K, consistent with a trivalent state of the $R$ ions. At lower temperature, magnetization and heat capacity measurements reveal antiferromagnetic ordering in $Gd_3Pt_4Ge_{13}$ ($T_N$ = 6.2 ± 0.1 K) and a ferromagnetic one in $Er_3Pt_4Ge_{13}$ ($T_C$ = 2.2 ± 0.1 K). $Dy_3Pt_4Ge_{13}$ presents a magnetic order at $T^*$ = 1.8 ± 0.2 K. $Ho_3Pt_4Ge_{13}$ behaves as a Van Vleck type paramagnet below 10 K and $Lu_3Pt_4Ge_{13}$ is found to be diamagnetic between 2 K and 300 K. This last compound shows no superconducting transition down to 400 mK.

**Keywords:** Intermetallic germanides, Rare earth compounds, High-pressure synthesis, Non-centrosymmetric crystal structure, Magnetism.

## 1. Introduction

*R-T-X* ternary intermetallic compounds, where *R* is a rare earth (or an alkaline earth), *T* a transition metal and *X* an element of groups 14 and 15, are a rich source of compounds where superconductivity and long-range magnetic order may coexist. The understanding of the fundamental mechanisms that govern this phenomenon remains a topical issue. Since the discovery in the middle of the seventies of superconductivity in rare earth-based Chevrel phases, $R_xMo_6S_8$, $R_xMo_6Se_8$ [1,2], tetraborides $(R)Rh_4B_4$ [3] or rhodium stannites $R_3Rh_4Sn_{13}$ [4], *R-T-X* ternary phase diagrams have been intensively explored [5,6]. Meanwhile a new series of defined compounds, filled skutterudites $RFe_4P_{12}$, was discovered [7]. The $RT_4X_{12}$ skutterudites are cage systems, where the icosahedral voids formed by the $T_4X_{12}$ framework

are filled with *R* ions. They have been synthesized with *T* = Fe, Ru, Os and *X* = P, Sb, As [8,9] and more recently with *T* = Pt and *X* = Ge [10,11] and have sparked off a great interest, not only as potential materials for thermoelectric applications [12], but also because they display a great wealth of non-conventional physical behaviours: metal-insulator transition, non-conventional superconductivity, coexistence of superconductivity and magnetic order, heavy-fermion behaviour, intermediate valence behaviour, … [10,11,13-16].

In filled skutterudites, the *X*-*X* bonding distances and the *X*-*T*-*X* angles deviate from their ideal values in order to accommodate the *R* ions. These deviations should become smaller when the size of the *R* ions decreases. However, when the size of the *R* ions is too small, depending on the *T* and *X* elements, the voids of the $T_4X_{12}$ framework may become too large to obtain optimal bonding distances and then competing phases become more stable. This difficulty can be overcome by using high-pressure synthesis and several skutterudite compounds filled with heavy *R* ions were prepared using this technique [17-20]. With the aim to synthesize skutterudites of the $RPt_4Ge_{12}$ series with heavy rare earths using the high-pressure high-temperature technique, Gumeniuk *et al.* found a new family of compounds, the composition of which, $R_3Pt_4Ge_{13}$, is reminiscent of that of rare earth rhodium stannites, $R_3Rh_4Sn_{13}$ [21]. $R_3Pt_4Ge_{13}$ have been reported to exist with *R* = Ca, Y, Pr, Sm, Gd, Tb, Tm and Yb [21-23]. It turns out that the crystal structures of these new compounds, though closely related to the cubic archetype structure $Yb_3Rh_4Sn_{13}$, differ from it through a variety of subtle structural distortions. These compounds exhibit a wide variety of structures and magnetic properties. The cubic $Ca_3Pt_4Ge_{13}$ compound (space group $I2_13$) is found to be diamagnetic [21]. The tetragonal compound $Yb_3Pt_4Ge_{13}$ (space group $P4_2cm$) features Yb in a temperature-independent non-magnetic $4f^{14}$ ($Yb^{2+}$) configuration [21]. The non-centrosymmetric (space group *Cc*) Y, Pr, Sm, Tb and Tm-based compounds are found to be, respectively, superconducting with $T_C$ = 4.5 K; magnetically ordered at 4.5 K and 4.0 K; Van Vleck type magnet; ferromagnetic at 4.0 K and paramagnetic down to 1.8 K. Surprisingly, for an ion with a zero orbital moment, $Gd_3Pt_4Ge_{13}$ presents two magnetic transitions at 6.3 K and 4.2 K [23].

In order to complete the results already published on this $R_3Pt_4Ge_{13}$ series, we have recently succeeded in synthesizing 4 new compounds with *R* = Dy, Ho, Er and Lu under high-pressure and high-temperature conditions. We report here on the determination of their crystal structure and magnetic properties. The $Gd_3Pt_4Ge_{13}$ compound, previously reported by R. Gumeniuk *et al.* [23], has been also prepared in order to clarify its magnetic behaviour at low temperature.

## 2. Sample synthesis

The precursor polycrystalline alloys of nominal composition $R_3Pt_4Ge_{13}$ were prepared by induction melting of the elements in a water-cooled copper crucible under a highly purified argon atmosphere. Elements are high-purity wires of platinum (Alfa Aesar, 99.95%), germanium (Goodfellow, 99.999%) and rare earths (Johnson Matthey, 99.9%) ingots. The pellets were melted several times to improve their homogeneity. It has been established that the mass losses after this first step are of the order of 1%. X-ray diffraction patterns measured using a conventional X-ray powder diffractometer (Philipps PW1730, Cu-Kα radiation) indicated that the thus produced samples were composed of $R$PtGe$_2$, PtGe$_2$ and Ge. To obtain the $R_3Pt_4Ge_{13}$ phases, with $R$ = Gd, Dy, Ho, Er and Lu, HP HT synthesis must be performed. Each sample was then grounded into a fine homogeneous powder and compacted under 1 kbar into cylindrical pellets of 3 mm diameter and a few mm in height. The pellets are then introduced into a crucible of hexagonal-boron nitride (h-BN).

The HP HT treatment was performed using a belt-type device fitted with a graphite tube furnace inserted in a pyrophyllite gasket, which serves as the pressure transmitting medium. A wide range of synthesis parameters was studied: pressure, temperature and dwell time were varied from 4 to 7 GPa, from 973 to 1173 K and from 30 minutes to 5h, respectively. The procedure for the HP HT treatment is the following: at room temperature the pressure is first applied, the temperature is then raised at a rate of 75 K/min up to the desired value. At the end of the annealing time, the sample is quenched by switching off the heating power. The pressure is then slowly reduced to the ambient value. All the samples could be easily separated from the crucible and subsequently powder X-ray diffraction measurements confirmed that there was no chemical reaction between the crucible and the samples.

The phase purity of the samples was also studied by field emission scanning electron metallography using a Field Emission gun Scanning Electron Microscope (FESEM-Zeiss Ultra plus microscope). It was found that the pure phase is obtained in a narrow window of pressure and temperature and that the HP HT conditions must be precisely adapted for each compound. This is illustrated for instance for $Er_3Pt_4Ge_{13}$ in figure 1. It was also found that the temperature should not exceed 1073 K, because above this temperature, a liquid phase forms and decreases the effect of the high-pressure as the BN crucible is not hermetically closed. Finally, time dependent tests show that, once the optimal values for pressure and temperature have been selected, one-hour annealing is enough to obtain the desired phase with a good purity.

The $R_3Pt_4Ge_{13}$ compounds with $R$ = Gd, Dy, Ho and Er were successfully synthetized at

T = 1073 ± 20 K under P = 5.0 ± 0.5 GPa. A higher pressure, P = 6.8 ± 0.5 GPa, and a lower temperature, T = 1023 ± 20 K, where required to obtain the $Lu_3Pt_4Ge_{13}$ phase. Purity of the samples was greater than 90%, except for the Lu-phase (80% pure) for which the maximum pressure available was not sufficient. The impurities that could be observed were composed of free Ge, $PtGe_2$ and $RPtGe_2$. Scanning electron microscopy (SEM) analysis revealed good homogeneity of the polycrystalline samples, as illustrated in figure 1-b in the case of $Er_3Pt_4Ge_{13}$.

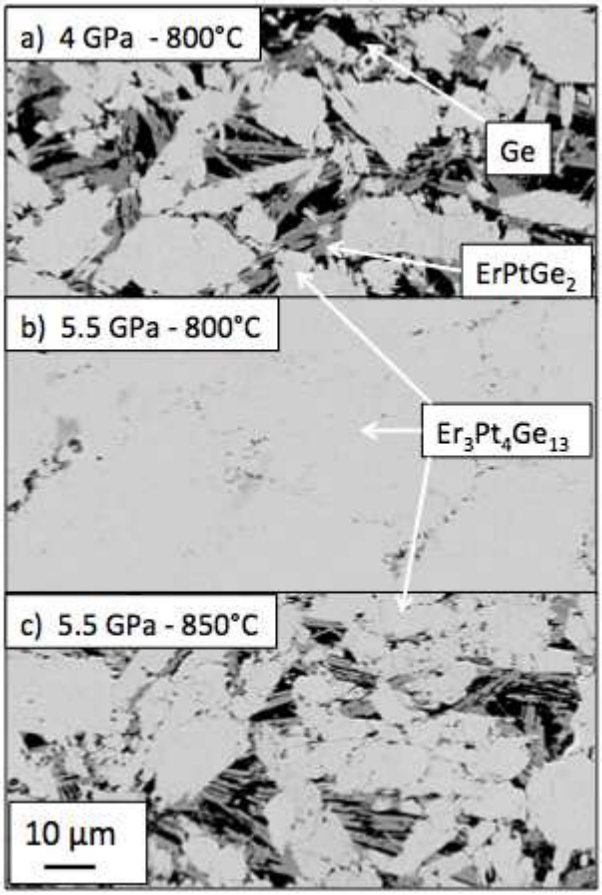


**Fig. 1.** Back scattered electron images of three tries of synthesis of $Er_3Pt_4Ge_{13}$ with different HP-HT conditions. These images are obtained under a voltage of 20 kV. Black, grey and light grey grains are composed of Ge, $ErPtGe_2$ and $Er_3Pt_4Ge_{13}$, respectively.

## 3. Crystal structure determination

The $R_3Pt_4Ge_{13}$ phases are metastable phases that were first synthesized by R. Gumeniuk *et al.* [23]. They showed that, depending on the *R* element, these phases crystallize with different structures of cubic, tetragonal, rhombohedral or monoclinic symmetry. On the basis of group-subgroup schemes, all these structures can be considered as derivatives of the initial $Yb_3Rh_4Sn_{13}$ cubic structure [23]. The HP-HT synthesized $R_3Pt_4Ge_{13}$ compounds with *R* = Pr,

Sm, Gd, Tm and Tb are reported to crystallize within a non-centrosymmetric monoclinic structure of space group *Cc*. This structure derives from the cubic one with $a_{mon.} \approx b_{mon.} \approx a_{cub.} \sqrt{2}$.

The powder X-ray patterns of all the compounds reported in this work are successfully indexed within the same monoclinic *Cc* space group, as illustrated in figure 2 for $Ho_3Pt_4Ge_{13}$. For this compound, the crystal structure was investigated by Rietveld refinement of the X-ray powder diffraction data using the FullProf program [24], starting from the structure reported by Gumeniuk *et al.* [22] for $Y_3Pt_4Ge_{13}$. All 20 atoms in the asymmetric unit occupy the general *4a* Wyckoff position, leading to a very large number of structural parameters. Given the limited number of Bragg reflections in the experimental X-ray pattern we did not attempt to refine atomic position parameters, which were kept fixed. A single isotropic atomic displacement parameter was refined for each atomic species, as well as the monoclinic cell parameters. A pseudo-Voigt function was used to describe the reflection profiles and the background was described by linear interpolation between selected points with refined intensity. The final refinements yielded the following agreement factors: $R_{wp}$=14.9, $Chi^2$= 1.94 and $R_{Bragg}$= 3.83. Attempts to refine the heavy Pt and Ho atom positions did not lead to a significant improvement and more extended data are required for a detailed structural investigation.

Based on the non-centrosymmetric monoclinic structure of space group *Cc*, the values of the lattice parameters for all the compounds were obtained by a LeBail type refinement (pattern matching refinement) of the X-ray powder diffraction data and are presented in table 1. One observes that the $R_{Bragg}$ factor obtained for $Lu_3Pt_4Ge_{13}$ is rather high compared to the other compounds. We ascribe this to the fact that the optimal conditions for the HP HT synthesis could not be reached with our setup for the $Lu_3Pt_4Ge_{13}$ phase. Consequently, the synthesis was not complete (20% impurity phases: $LuPtGe_2$, $PtGe_2$ and Ge).

These value are compared in figure 3 with those previously reported by Gumeniuk *et al.* [22,23] for the $R_3Pt_4Ge_{13}$ compounds with *R* = Pr, Sm, Gd, Tm and Tb.

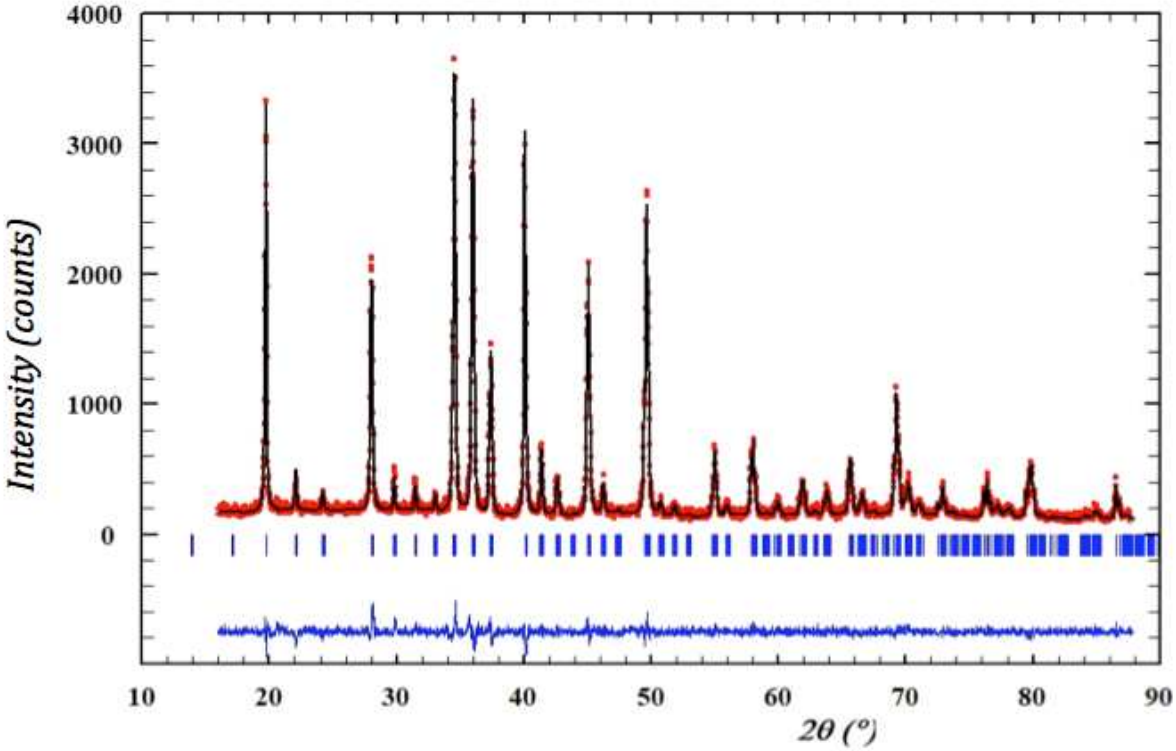


**Fig. 2.** Experimental (red circles) and calculated (black line) powder XRD pattern of the $Ho_3Pt_4Ge_{13}$ phase. Bragg peak positions, based on the monoclinic non-centrosymetric *Cc* space group, are given by the blue sticks. The difference plot has been calculated and is given by the blue curve displayed at the bottom of the figure.

**Table 1**

Refined lattice parameters for the $R_3Pt_4Ge_{13}$ compounds with *R* = Gd, Dy, Ho, Er and Lu. The value of the Bragg agreement factor, $R_{Bragg} = \frac{\Sigma_i|I_i^{obs} - I_i^{cal}|}{\Sigma_i|I_i^{obs}|}$, is given in the last column.

| Compound | a (Å) | b (Å) | c (Å) | β (°) | $R_{Bragg}$ |
|---|---|---|---|---|---|
| $Gd_3Pt_4Ge_{13}$ | 12.7920(7) | 12.7733(5) | 9.0389(4) | 88.581(4) | 1.22 |
| $Dy_3Pt_4Ge_{13}$ | 12.7400(4) | 12.7042(4) | 8.9987(2) | 89.764(3) | 0.84 |
| $Ho_3Pt_4Ge_{13}$ | 12.7374(2) | 12.6951(2) | 8.9928(3) | 89.752(2) | 0.64 |
| $Er_3Pt_4Ge_{13}$ | 12.7188(4) | 12.6768(4) | 8.9858(3) | 89.732(2) | 0.88 |
| $Lu_3Pt_4Ge_{13}$ | 12.698(3) | 12.645(3) | 8.946(3) | 89.67(2) | 2.13 |

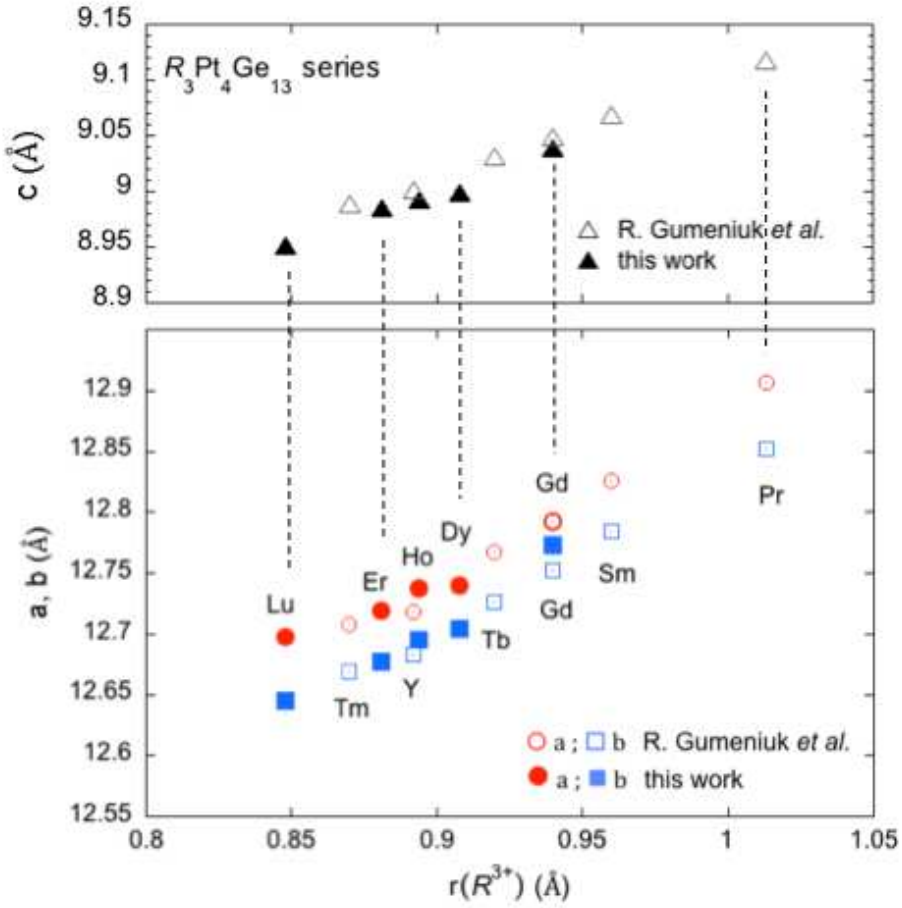


**Fig. 3.** Evolution of the lattice parameters: a, b, c, in the monoclinic (*Cc* space group) $R_3Pt_4Ge_{13}$ series with the radius of the $R^{3+}$ ion given by R.D. Shannon in Ref. [25]. The corresponding *R* element has been specified and the dotted lines are just guides for the eye. Our data are compared with those reported in Ref. [22] and [23] for other compounds of the same series.

As shown in figure 3, the lattice parameters of the compounds studied in this work are consistent with those previously reported by R. Gumeniuk *et al.* [22,23] for other compounds of the same series. The decrease of the a, b and c values with the decrease of the radius of the trivalent rare earth ion is in full agreement with the lanthanide contraction effect [26]. This effect is mainly due to an incomplete shielding of the nuclear charge by the 4*f* electrons, although the 4*f* orbitals are rather compact in shape. Such behaviour has already been observed in many rare-earth series. The *Cc* structure being a derivative of the cubic *Pm*-3*n* one, a comparison of the observed lanthanide contraction with the germanides $R_3Ir_4Ge_{13}$ series can be made. From data published in the literature, the relative variation of the cell volume $\Delta V/V$ is equal to -5.1 % (from Pr- to $Lu_3Ir_4Ge_{13}$ [27]). This value is perfectly consistent with -4.9 % found in the case of the $R_3Pt_4Ge_{13}$ series (from the Pr to the Lu based compounds, [23] and this work).

Except for $Gd_3Pt_4Ge_{13}$, it is observed that the value of the β angle decreases when going from the Dy to the Lu compounds (see Table 1). This progressive distortion of the *Cc* structure is very likely related to the lanthanide contraction effect. It is clearly noticeable on the rare earth environment with the form of the distorted $RPt_{12}$ icosahedral polyhedrons and also on the platinum environment with the distortion of the $PtGe_6$ trigonal prisms, as illustrated by the two representations in figure 4.

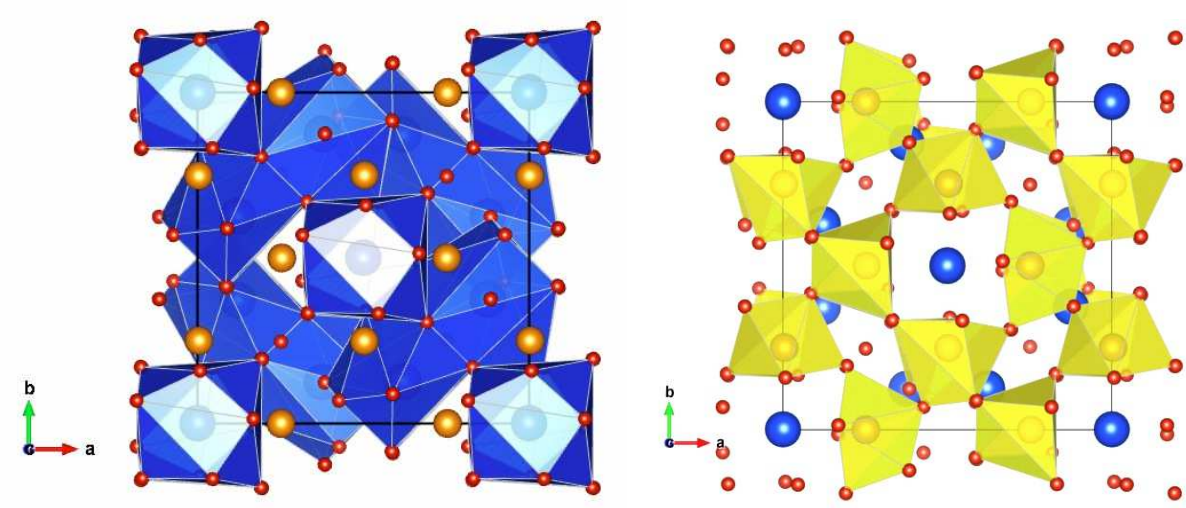


**Fig. 4 .** Representation of the $R_3Pt_4Ge_{13}$ crystal structure based on the *Cc* space group and the atomic coordinate information published by R. Gumeniuk *et al.* [21]. Ge atoms are represented by small red spheres, Pt atoms by orange intermediate spheres and *R* atoms by large blue spheres. Left: representation of the Ge icosahedral polyhedrons surrounding the *R* atoms and right: representation of the Ge trigonal prims surrounding the Pt atoms.

## 4. Magnetic properties and heat capacity measurements

Magnetic characterization of the compounds was carried out on a commercial Quantum Design MPMS magnetometer using the reciprocating sample option (RSO). The magnetic signal is recorded with the sample oscillating around the centre of the SQUID pickup coils and it is fitted to an ideal dipole response using a non-linear least-square routine.

The sample holders are made out of a plastic straw. As the dimensions of the samples are smaller than the straw diameter, they are wrapped in a thin plastic membrane that allows the sample to be held in position inside the straw. For samples presenting very weak magnetic signals, typically between $-10^{-5}$ and $+10^{-5}$ emu, data are corrected from the contribution of the sample holder. This contribution is obtained by measuring the empty plastic membrane mounted inside the straw, with exactly the same geometry as when measuring the sample. In the present study, correction is needed only for the $Lu_3Pt_4Ge_{13}$ compound.

For $Gd_3Pt_4Ge_{13}$, $Dy_3Pt_4Ge_{13}$, $Ho_3Pt_4Ge_{13}$ and $Er_3Pt_4Ge_{13}$, isothermal magnetization curves, M(H), were measured in the temperature range 2 K-300 K. The same sequence of

measurements has been used for all samples. The sample is first cooled down to the base temperature of the magnetometer in zero field, then the magnetic measurements are performed while increasing the temperature. Once the temperature is stabilised at the desired value, the magnetization is measured while varying the field from 0 to 50 kOe. The field is then set to zero and the temperature is raised to the new desired value. The inverse magnetic susceptibility was deduced from Arrott plots, $M^2 = f(H/M)$ [28].

The thermal variation of the isofield magnetization, M(T), has also been measured in all these compounds in zero field-cooled and field-cooled procedures. M(T) curves have been recorded under different fields: 500, 2000 and 5000 Oe, in order to check that the inverse magnetic susceptibility, deduced from the H/M(T) curves, is consistent with that deduced from the Arrott plots.

The thermal variation of the experimental inverse susceptibilities of $Gd_3Pt_4Ge_{13}$, $Dy_3Pt_4Ge_{13}$, $Ho_3Pt_4Ge_{13}$ and $Er_3Pt_4Ge_{13}$ are shown in figure 5. For all these compounds, above 10 K the inverse susceptibility varies linearly with temperature. Since 4*f* ions bear a very localised magnetic moment, in rare earth-based intermetallics the magnetic susceptibility obeys the Curie-Weiss law. The inverse susceptibility is given by $\frac{1}{\chi} = \frac{T}{C} - n_{ex}$, where $C$ is the Curie constant of the rare earth ion of total angular momentum *J*, $C = N_A \frac{g_J^2 J(J+1)\mu_B^2}{3k_B}$ per mole of rare earth and $n_{ex}$ is the exchange constant that accounts for exchange interactions between the 4*f* magnetic moments. $n_{ex}$ and the paramagnetic Curie temperature, $\theta_p$, are related by $n_{ex} = \theta_p / C$. In the presence of exchange interactions, the inverse susceptibility remains parallel to the inverse Curie susceptibility, $\frac{1}{\chi} = \frac{T}{C}$, but is shifted by $n_{ex}$. The black lines in figure 5 represent the inverse susceptibilities calculated for trivalent rare earth ions using the Curie-Weiss law. The best agreement between experimental and calculated reciprocal susceptibilities is obtained for the values of $n_{ex}$ given in table 2. The signs of $n_{ex}$ indicate antiferromagnetic correlations in $Gd_3Pt_4Ge_{13}$, $Dy_3Pt_4Ge_{13}$ and $Ho_3Pt_4Ge_{13}$ and ferromagnetic correlations in $Er_3Pt_4Ge_{13}$. The largest absolute exchange constant is found in the Gd compound. This is consistent with the fact that the $Gd^{3+}$ ion bears the largest spin (S = 7/2) in the lanthanide series.

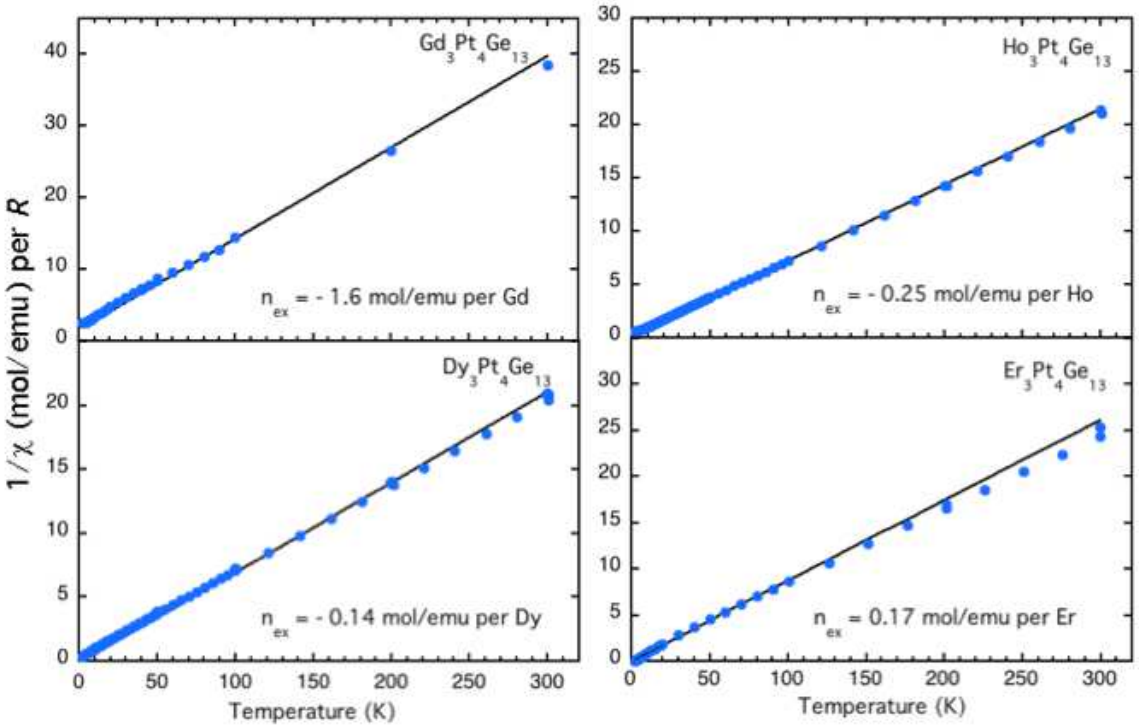


**Fig. 5.** Thermal variation of the inverse magnetic susceptibility of $Gd_3Pt_4Ge_{13}$, $Dy_3Pt_4Ge_{13}$, $Ho_3Pt_4Ge_{13}$ and $Er_3Pt_4Ge_{13}$ deduced from magnetization curves measured at 500 Oe. The black line is the inverse susceptibility calculated for the trivalent rare earth ion using the Curie-Weiss law: $\frac{1}{\chi} = \frac{T}{C} - n_{ex}$. The values of Curie constants *C* used are given in table 2.

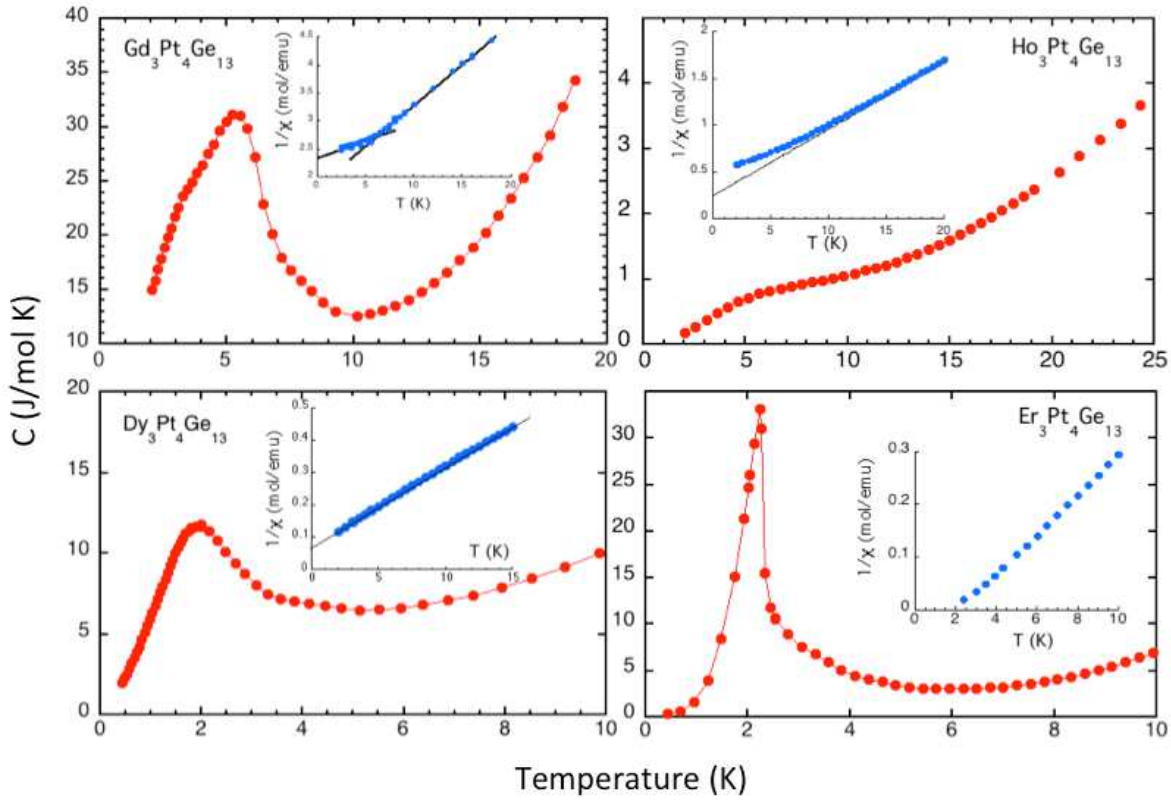


**Fig. 6.** Low temperature domain: thermal variation of the specific heat and the inverse magnetic susceptibility (inset) of the $Gd_3Pt_4Ge_{13}$, $Dy_3Pt_4Ge_{13}$, $Ho_3Pt_4Ge_{13}$ and $Er_3Pt_4Ge_{13}$ compounds. Note that the inverse susceptibility is given in mol/emu per *R* element (same units as for figure 5).

The heat capacity was measured using the relaxation method on a commercial Quantum Design PPMS in the temperature range 400 mK - 300 K. Figure 6 compares the thermal variation of the specific heat and the inverse magnetic susceptibility in the low temperature range (T < 20 K) for the Gd, Dy, Ho and Er compounds.

In $Er_3Pt_4Ge_{13}$, a well-defined λ-type anomaly is observed in the specific heat just above 2 K while the inverse susceptibility intersects the temperature axis at 2.2 K. This confirms the onset of ferromagnetic order at $T_C = 2.2 \pm 0.1$ K.

For $Ho_3Pt_4Ge_{13}$, no lambda-type anomaly is observed in the specific heat curve down to 2 K. Instead, it shows a weak and wide hump at around 6 K. In the same temperature range, just below 10 K, the inverse susceptibility deviates from the Curie-law and tends to saturate toward a value of 0.5 mol/emu per Ho.
In rare earth compounds where the kinetic orbital momentum is not zero, crystalline electric field (CEF) effects lead to splitting of the ground state multiplet *J*. Accordingly, the expression of the susceptibility must be modified by adding a new term that accounts for thermal effects on the CEF levels. This second term is called the Van Vleck term. When the CEF ground state is non-magnetic, which is very often the case for non-Kramers ions such as $Ho^{3+}$, the Curie term in the susceptibility vanishes when the temperature is decreased, while, through the Van Vleck term the susceptibility (and hence its reciprocal) tends toward a finite value. Due to the low point symmetry of the rare earth site in the $R_3Pt_4Ge_{13}$ series, the CEF effects split the $J = 8$ multiplet of $Ho^{3+}$ into 17 non-magnetic singlets. This explains the Van Vleck-type paramagnetic behaviour of the magnetic susceptibility at low temperature. The hump in the specific heat is likely a Schottky anomaly resulting from the population of excited CEF levels.

The specific heat curves of $Gd_3Pt_4Ge_{13}$ and $Dy_3Pt_4Ge_{13}$ show rather broad anomalies around 6 K and 1.8 K respectively. This shape of the specific heat is very reminiscent of features observed in several rare earth intermetallic compounds such as $GdNi_2Si_2$, $GdGa_2$, $GdCu_5$ [29] or $PrNi_2Si_2$ [30]. These very peculiar features have been explained by the occurrence of incommensurate amplitude modulated magnetic structures in these compounds [31]. Incommensurate magnetic structures are particularly common in rare earth intermetallic compounds where the oscillatory character of the long-range RKKY-type exchange coupling leads to antagonistic interactions and hence to frustration. The change of slope of the $Gd_3Pt_4Ge_{13}$ inverse susceptibility curve at 6.2 K bears evidence of the existence of a magnetic

transition. This and the very particular shape of the specific heat anomaly are indicative of a phase transition towards an incommensurate magnetic structure. In the case of $Dy_3Pt_4Ge_{13}$, although the thermal variation of the inverse susceptibility reveals no anomaly down to 2 K, the base temperature of the magnetometer, it is also likely that the specific heat anomaly at T* = 1.8 ± 0.2 K is related to a magnetic phase transition. According to the negative sign of the exchange constant $n_{ex}$, it can be inferred that this phase is antiferromagnetic. Nonetheless, this should be confirmed by further magnetic measurements at lower temperature. Table 2 summarizes the order temperatures obtained either by magnetic or specific heat measurements.

**Table 2**
Magnetic characteristics overview for the Gd, Dy, Ho and Er based compounds. The value of the theoretical Curie constant used in the Curie Weiss law (see text) is given in the last column.

| **Compounds** | **$n_{ex}$ (mol/emu per *R*)** | **$T_{order}$ (K)** | **Curie constant (emu K/mol)** |
|---|---|---|---|
| $Gd_3Pt_4Ge_{13}$ | -1.6 ± 0.2 | $T_N$ = 6.2 ± 0.1 | 7.880 |
| $Dy_3Pt_4Ge_{13}$ | - 0.14 ± 0.05 | T* = 1.8 ± 0.2 | 14.125 |
| $Ho_3Pt_4Ge_{13}$ | - 0.25 ± 0.05 | - | 14.045 |
| $Er_3Pt_4Ge_{13}$ | + 0.17 ± 0.05 | $T_C$ = 2.2 ± 0.1 | 11.496 |

In $Lu^{3+}$ ions the 4*f* shell is full thus no net magnetic moment is expected on these ions in the $Lu_3Pt_4Ge_{13}$ compound. For this compound only measurements of the thermal variation of the isofield magnetization, M(T), have been performed. Because of the weak magnetic signal of this compound, the measurements have been carried out under an applied field of 50 kOe.

As shown in figure 7, the $Lu_3Pt_4Ge_{13}$ compound is found to be diamagnetic down to 2 K. A diamagnetic susceptibility of $\chi$ = -7.2±0.1 $10^{-4}$ emu/mol has been deduced from the linear fit of the $\chi \cdot T = f(T)$ curve in the temperature range 50-300 K. This value is comparable to that of diamagnetic $Y_3Pt_4Ge_{13}$ ($\chi$ = -3.67 $10^{-4}$ emu/mol) [22]. Below 30 K, the susceptibility (not shown here) shows an upturn and starts increasing. In weak magnetic or non-magnetic systems, small amounts of diluted magnetic impurities lead to signals the intensity of which are comparable to that of the compound. This pollution can be hardly avoided even using highly purified elements and/or working in very controlled atmospheres, especially when the compound is subjected to many handlings, as is the case for HP HT synthesis. Iron and iron oxides are the most frequent source

of magnetic contamination. We thus tried to account for the low temperature tail assuming $Fe^{2+}$ ($\mu_{eff}$ = 5.4 $\mu_B$) impurities. This leads to a mass concentration lower than 0.02%.

The specific heat shows no anomaly down to 400 mK. From the $C/T = \gamma + \beta T^2$ curve (inset figure 7), the Sommerfeld coefficient has been determined, $\gamma$ = 18.5 mJ / (mol $K^2$). The slope of the curve gives $\beta$ = 3.8 mJ / (mol $K^4$) which leads to a Debye temperature $\theta_D$ = 217 K. All these values are in good agreement with those reported for $Y_3Pt_4Ge_{13}$ ($\gamma$ = 19 mJ / (mol $K^2$) and $\theta_D$ = 257 K [22]).

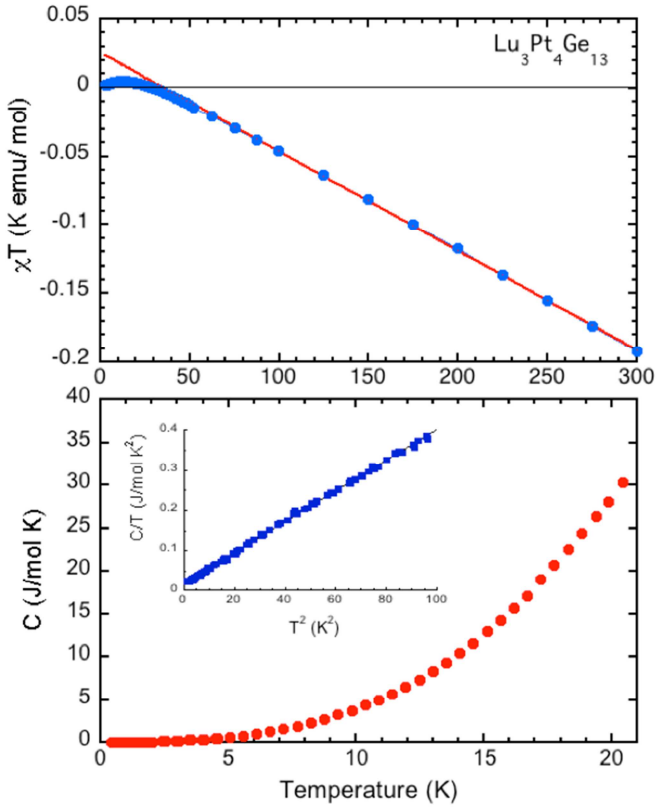


**Fig. 7.** Top: $\chi$.T versus T where $\chi$ is the magnetic susceptibility of $Lu_3Pt_4Ge_{13}$ measured at 50 kOe and given in emu per mol of compound. The full line corresponds to the linear fit in the temperature range 50-300 K. The slope gives a diamagnetic susceptibility $\chi$ = -7.2±0.1 $10^{-4}$ emu/mol. Bottom: thermal dependence of the specific heat down to 400 mK. The inset shows the linear behaviour of C/T versus $T^2$ in the temperature range: 400 mK – 10 K.

Figure 8 compares the evolution of the ordering temperatures with the de Gennes factor $dG = (g_J - 1)^2 J(J+1)$, in the heavy rare earth side of the $R_3Pt_4Ge_{13}$ series. Note that $Ho_3Pt_4Ge_{13}$ behaves as a Van Vleck paramagnet at low temperatures and hence does not order magnetically. For $Tm_3Pt_4Ge_{13}$ no magnetic order was detected above 1.8 K [23]. The Yb compound cannot be included in this scheme as it crystallizes in a tetragonal structure ($P4_2mc$ space group) [21]. The values of the ordering temperatures decrease from the Gd compound. Such behaviour is very similar to that reported for many other rare earth-based intermetallic

series [27,32-34]. Except for the Er based compound, the ordering temperatures scale rather well with the de Gennes law [35], as expected for RKKY-type exchange interactions between localised magnetic moments. However, de Gennes scaling does not take into account CEF effects in the effective exchange parameter [36]. Further investigations in the evolution of the crystal-field parameters should explain the deviation to the de Gennes law observed for the Er based compound.

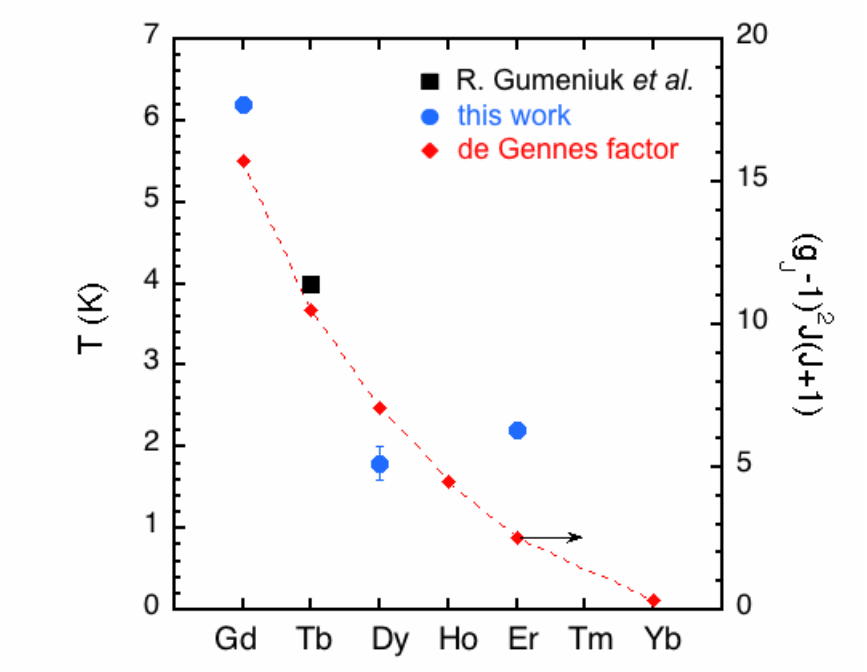


**Fig. 8.** Comparison between the experimental ordering temperatures (dots and square) and the de Gennes factor (diamonds connected by the dotted line) in the heavy rare earth side of the $R_3Pt_4Ge_{13}$ series. $Ho_3Pt_4Ge_{13}$ is a Van Vleck paramagnet at low temperature and no magnetic order has been observed down to 1.8 K in $Tm_3Pt_4Ge_{13}$ [23].

## 6. Conclusion

The existence of non-centrosymmetric compounds of composition $R_3Pt_4Ge_{13}$ was first reported by Gumeniuk *et al.* [22,23]. In the present work we have shown that this series, which crystallises within the *Cc* space group, can be fully completed in the heavy rare earth side up to the Lu based compound. It is demonstrated that the high-pressure high-temperature synthesis parameters need to be adapted for each compound, according to the progressive decrease of the rare earth ionic radius.

From specific heat and magnetic measurements, we have shown that $Gd_3Pt_4Ge_{13}$ orders anti-ferromagnetically at 6.2 K, whereas $Er_3Pt_4Ge_{13}$ orders ferromagnetically under 2.2 K. From specific heat measurements, $Dy_3Pt_4Ge_{13}$ shows a transition temperature at 1.8 K, which is probably related to an antiferromagnetic order. However, the real nature of this order needs to be confirmed by further magnetic measurements at temperatures lower than 2K. $Ho_3Pt_4Ge_{13}$

shows a Van Vleck behaviour and finally, $Lu_3Pt_4Ge_{13}$ is diamagnetic.

Despite the fact that the non-magnetic $Lu_3Pt_4Ge_{13}$ compound does not reveal superconductivity, the value of its Sommerfeld coefficient is comparable to that of $Y_3Pt_4Ge_{13}$, which becomes superconducting below $T_c = 4.5$ K [22].

Except for the Er based compound, the ordering temperatures of the heavy rare earth side in this $R_3Pt_4Ge_{13}$ series follow rather well the de Gennes law [35].

**Acknowledgments**

We greatly acknowledge technical assistance from A. Hadj-Azzem, J. Balay, Y. Deschanels, D. Dufeu, E. Eyraud and P. Lachkar, all from Institut Néel.

**References**

[1] O. Fischer, A. Treyvaud, R. Chevrel and M. Sergent, Sol. St. Comm. **17** (1975) 721.

[2] R. N. Shelton, R. W. McCallum and H. Adrian, Phys. Lett. A **56** (1976) 213.

[3] B. T. Matthias, E. Corenzwit, J. M. Vandenberd and H. Barz, Proc. Natl. Acad. Sci. USA **74** (1977) 1334.

[4] J. P. Remeika, G. P. Espinosa, A. S. Cooper, H. Barz, J. M. Rowell, D. B. McWhan, J. M. Vandenberg, D. E. Moncton, Z. Fisk, L. D. Woolf, H. C. Hamaker, M. B. Maple, G. Shirane, W. Thomlinson, Sol. St. Comm. **34** (1980) 923.

[5] K. Ghosh, S. Ramakrishnan and G. Chandra, Phys. Rev. B **48** (1993) 10435.

[6] B. K. Rai, I. W. H. Oswald, J. K. Wang, G. T. McCandless, J. Y. Chan and E. Morosan, Chem. Mat. **27** (2015) 2488.

[7] W. Jeitschko and D. J. Braun, Acta Cryst. B **33** (1977) 3401.

[8] D. J. Braun and W. Jeitschko, J. Less-Common Met. **72** (1980) 147.

[9] I. Shirotani, T. Uchiumi, K. Ohno, C. Sekine, Y. Nakazawa, K. Kanoda, S. Todo, and T. Yagi, Phys. Rev. B **56** (1997) 7866.

[10] E. Bauer, A. Grytsiv, Xing-Qiu Chen, N. Melnychenko-Koblyuk, G. Hilscher, H. Kaldarar, H. Michor, E. Royanian, G. Giester, M. Rotter, R. Podloucky and P. Rogl, Phys. Rev. Lett. **99** (2007) 217001.

[11] R. Gumeniuk, W. Schnelle, H. Rosner, M. Nicklas, A. Leithe-Jasper and Y. Grin, Phys. Rev. Lett. **100** (2008) 017002.

[12] C. Uher, Semiconductors and Semimetals, Vol. **69** (Academic Press, New York, 2001), p. 139.

[13] C. Sekine, T. Uchiumi and I. Shirotani, Phys. Rev. Lett. **79** (1997) 3218.

[14] E. D. Bauer, N. A. Frederick, P.-C. Ho, V. S. Zapf, and M. B. Maple, Phys. Rev. B **65** (2002) 100506 (R).

[15] K. Kuwahara, K. Iwasa, M. Kohgi, K. Kaneko, N. Metoki, S. Raymond, M.-A. Measson, J. Flouquet, H. Sugawara, Y. Aoki and H. Sato, Phys. Rev. Lett. **95** (2005) 107003.

[16] R. Gumeniuk, K. O. Kvashnina, W. Schnelle, M. Nicklas, H. Borrmann, H. Rosner, Y. Skourski, A. A. Tsirlin, A. Leithe-Jasper and Y. Grin, J. Phys.: Condens Matter **23** (2011) 465601.

[17] C. Sekine, T. Uchiumi, I. Shirotani, K. Matsuhira, T. Sakakibara, T. Goto, and T. Yagi, Phys. Rev. B **62** (2000) 11581.

[18] K. Kihou, I. Shirotani, Y. Shimaya, C. Sekine, T.Yag, Mat. Res. Bull. **39** (2004) 317.

[19] I. Shirotani, N. Araseki, Y. Shimaya, R. Nakata, K. Kihou, C. Sekine and T.Yagi, J. Phys.: Condens. Matter **17** (2005) 4383.

[20] R. Gumeniuk, M. Schöneich, A. Leithe-Jasper, W. Schnelle, M. Nicklas, H. Rosner, A. Ormeci, U. Burkhardt, M. Schmidt, U. Schwarz, M. Ruck and Yu Grin, New J. Phys. **12** (2010) 103035.

[21] R. Gumeniuk, L. Akselrud, K. O. Kvashnina, W. Schnelle, A. A. Tsirlin, C. Curfs, H. Rosner, M. Schöneich, U. Burkhard, U. Schwarz, Y. Grin and A. Leithe-Jasper, Dalton Trans. **41** (2012) 6299.

[22] R. Gumeniuk, M. Nicklas, L. Akselrud, W. Schnelle, U. Schwarz, A. A. Tsirlin, A. Leithe-Jasper and Y. Grin, Phys. Rev. B **87** (2013) 224502.

[23] R. Gumeniuk, M. Schöneich, K. O. Kvashnina, L. Akselrud, A. A. Tsirlin, M. Nicklas, W. Schnelle, O. Janson, Q. Zheng, C. Curfs, U. Burkhard, U. Schwarz and A. Leithe-Jasper, Dalton Trans. **44** (2015) 5638.

[24] J. Rodriguez-Carvajal, Satellite Meeting on Powder Diffraction of the XV Congress of the IUCr, Book of Abstracts, Toulouse, France (1990) 127.

[25] R. D. Shannon. Acta Cryst. A **32** (1976) 751.

[26] P. S. Bagus, Y. S. Lee and K. S. Pitzer, Chem. Phys. Lett. **33** (1975) 408.

[27] G. Venturini, M. Méot-Meyer, B. Malaman et B. Roques, J. Less-Common Met. 113 (1985) 197 - 204.

[28] A. Arrott, Phys. Rev. **108** (1957) 1394.

[29] M. Bouvier, P. Lethuillier, and D. Schmitt, Phys. Rev. B **43** (1991) 13137.

[30] J. A. Blanco, D. Schmitt and J.C. Gomez Sal, J. Magn. Magn. Mater. **116** (1992) 128.

[31] J. A. Blanco, D. Gignoux and D. Schmitt, Phys. Rev. B **43** (1991) 13145.

[32] C. Opagiste, C. Barbier, R. Heattel and R. M. Galéra, J. Magn. Magn. Mater. **378** (2015) 402.

[33] P. C. Canfield, P.L. Gammel and J. Bishop, Phys. Today **51** (1998) 40.

[34] A. M. Tishin, J. Alloys Compd. **250** (1997) 635.

[35] P. G. de Gennes, C. R. Acad. Sci. **247** (1959) 1836.

[36] B. Coqblin, The Electronic Structure of Rare-Earth Metal and Alloys: The Magnetic Heavy Rare Earths - Academic Press, New York, 1977.